# Magnetic-sublevel-independent magic wavelengths: Application to Rb and Cs atoms

Sukhjit Singh,[1,*] B. K. Sahoo,[2,†] and Bindiya Arora[1,‡]
[1]*Department of Physics, Guru Nanak Dev University, Amritsar, Punjab-143005, India*
[2]*Theoretical Physics Division, Physical Research Laboratory, Navrangpura, Ahmedabad-380009, India*
(Received 6 April 2016; published 24 June 2016)

A generic scheme to trap atoms at the magic wavelengths $\lambda_{\text{magic}}$ that are independent of vector and tensor components of the interactions of the atoms with the external electric field is presented. The $\lambda_{\text{magic}}$ for the laser cooling $D_2$ lines in the Rb and Cs atoms are demonstrated and their corresponding polarizability values without vector and tensor contributions are given. Consequently, these $\lambda_{\text{magic}}$ are independent of magnetic sublevels and hyperfine levels of the atomic states involved in the transition, thus, they can offer unique approaches to carrying out many high-precision measurements with minimal systematics. Inevitably, the proposed technique can also be used for electronic or hyperfine transitions in other atomic systems.

DOI: 10.1103/PhysRevA.93.063422

## I. INTRODUCTION

Techniques to cool and trap atoms using laser light have revolutionized modern experimental procedures. They are applied not only to carry out very high precision spectroscopy measurements, but also to probe many subtle signatures like parity violation [1], Lorentz symmetry invariance [2], and quantum phase transitions [3]. Vogl and Weitz demonstrated the cooling of Rb atoms by resonating the trap laser light with their $D$ lines [4], while Monroe *et al.* observed the clock transition in Cs by cooling the atom using the $D_2$ line [5]. As demonstrated in Ref. [6], trapping atoms at $\lambda_{\text{magic}}$ is the foremost process today in a number of applications such as constructing optical lattice clocks. Following this, a number of experimental and theoretical studies have been reported $\lambda_{\text{magic}}$ in the neutral atoms [7–14], and recently in the singly charged alkaline-earth-metal ions [15,16]. In a remarkable work, Katori *et al.* [17] demonstrated the use of magic wavelengths $\lambda_{\text{magic}}$ for Sr atoms to reduce the systematics in the measurements. Using $\lambda_{\text{magic}}$ for trapping and controlling atoms inside high-$Q$ cavities in the strong coupling regime with minimum decoherence for the $D_2$ line of Cs atom has been demonstrated by McKeever *et al.* [18]. Liu and co-workers experimentally demonstrated the existence of $\lambda_{\text{magic}}$ for the $^{40}Ca^{+}$ clock transitions [19].

A linearly polarized light is predominantly used to trap atoms, which is free from the contribution of the vector component of the interaction between atomic states and electric fields. A substantial drawback of these $\lambda_{\text{magic}}$ is that they are magnetic-sublevel dependent for the transitions involving states with angular momenta greater than 1/2. It has also been argued that considering circularly polarized light for trapping could be advantageous due to the dominant role played by the vector polarizability in the ac-Stark shift [9,20]. This may help in augmenting the number of $\lambda_{\text{magic}}$ in some cases but at the same time requires magnetic-sublevel selective trapping. The dependence of magic wavelengths on magnetic sublevels demands the need for state selective traps. To circumvent this problem, it is imperative to find $\lambda_{\text{magic}}$ that are independent of magnetic sublevels.

In this paper, we propose a scheme to trap atoms and ions at the $\lambda_{\text{magic}}$ that are independent of the atomic magnetic and hyperfine levels. They can be used in a number of the applications discussed above. Just for demonstration purposes, we present here $\lambda_{\text{magic}}$ of the widely used $D_2$ transitions of the Rb and Cs atoms. They are useful for optical communications where lasers are tuned to their $D$ lines to trap and repump the atoms in order to prevent them from accumulating in the ground state [21]. Moreover, $D_2$ lines of Rb and Cs are used for studying their microwave spectroscopy [4,5,22,23] and quantum logic gates [24], and to assert the accuracy of the fine structure constant [25]. In this proposal, we only presume that the atomic systems are trapped in sufficiently strong magnetic fields.

## II. THEORY

The ac-Stark shift for any state with angular momentum $K$ of an atom placed in an oscillating electric field $\vec{\mathcal{E}} = \frac{1}{2}\mathcal{E}\hat{\epsilon}e^{-\iota\omega t} + \text{c.c.}$ with polarization vector $\hat{\epsilon}$ is given as [26]

$$\Delta E_K = -\tfrac{1}{2}\alpha_K(\omega)\mathcal{E}^2, \tag{1}$$

where $\alpha_K(\omega)$ is the total dynamic polarizability for the state $K$ with its magnetic projection $M$ as

$$\alpha_K(\omega) = \alpha_K^{(0)}(\omega) + \beta(\epsilon)\frac{M}{2K}\alpha_K^{(1)}(\omega) + \gamma(\epsilon)\frac{3M^2 - K(K+1)}{K(2K-1)}\alpha_K^{(2)}(\omega), \tag{2}$$

where $\alpha_K^{(i)}(\omega)$ with $i = 0,1,2$ are the scalar, vector, and tensor components of the frequency-dependent polarizability respectively. In the above expression $K$ and $M$ can be replaced suitably by either the atomic angular momentum $J$ or hyperfine angular momentum $F$ with their corresponding magnetic projection $M_J$ or $M_F$, depending upon the consideration of atomic or hyperfine states, respectively. The $\beta(\epsilon)$ and $\gamma(\epsilon)$ are defined as [27]

$$\beta(\epsilon) = \iota(\hat{\epsilon} \times \hat{\epsilon}^*) \cdot \hat{\epsilon}_B, \tag{3}$$

*sukhjitphy.rsh@gndu.ac.in
†bijaya@prl.res.in
‡bindiya.phy@gndu.ac.in

 

and

$$\gamma(\epsilon) = \tfrac{1}{2}[3(\hat{\epsilon}^* \cdot \hat{e}_B)(\hat{\epsilon} \cdot \hat{e}_B) - 1], \tag{4}$$

with the quantization axis unit vector $\hat{e}_B$. The differential Stark shift of a transition between states $K$ to $K'$ is, hence, given by

$$\begin{aligned}\delta E_{KK'} = \Delta E_K - \Delta E_{K'} = -\frac{1}{2}\Bigg[&\left\{\alpha_K^{(0)}(\omega) - \alpha_{K'}^{(0)}(\omega)\right\} \\ &+\beta(\epsilon)\left\{\frac{M}{2K}\alpha_K^{(1)}(\omega) - \frac{M'}{2K'}\alpha_{K'}^{(1)}(\omega)\right\} \\ &+\gamma(\epsilon)\Bigg\{\frac{3M^2 - K(K+1)}{K(2K-1)}\alpha_K^{(2)}(\omega) \\ &-\frac{3M'^2 - K'(K'+1)}{K'(2K'-1)}\alpha_{K'}^{(2)}(\omega)\Bigg\}\Bigg]\mathcal{E}^2, \end{aligned} \tag{5}$$

It is obvious from the above expression that for obtaining null differential Stark shift, it is necessary that either independent components cancel out each other or the net contribution nullifies, which prominently depends on the choices of $M$, $\beta(\epsilon)$, and $\gamma(\epsilon)$ values. By adequately selecting the experimental configuration such that the $\beta(\epsilon)$ and $\gamma(\epsilon)$ values are zero, it is possible to remove the vector and tensor components. As implied from the above considerations and Eq. (5), the differential ac-Stark shift depends only on the scalar polarizabilities of the associated states. Thus, it is independent of the magnetic sublevels. Moreover, the scalar polarizabilities are the same for the atomic and hyperfine levels; i.e., $\alpha_J^{(0)} = \alpha_F^{(0)}$ (for all the allowed $F$ values). Hence, these $\lambda_{\text{magic}}$ are also independent of the hyperfine splittings of the participating atomic states. Therefore, $\lambda_{\text{magic}}$ obtained by applying the above conditions will be independent of the choice of $M_J$, $F$, and $M_F$ quantum numbers. On account of the above, we elucidate a laboratory frame in which null values for $\beta(\epsilon)$ and $\gamma(\epsilon)$ can be accomplished.

## III. DISCUSSION

We start our analysis by defining a coordinate system with the components $\hat{\epsilon}_{\text{maj}}$, $\hat{\epsilon}_{\text{min}}$, and $\hat{k}$, where $\hat{\epsilon}_{\text{maj}}$ and $\hat{\epsilon}_{\text{min}}$ are the real components of the complex unit polarization vector $\hat{\epsilon}$ and describe the system such that

$$\hat{\epsilon} = e^{\iota\sigma}(\cos\phi\hat{\epsilon}_{\text{maj}} + \iota\sin\phi\hat{\epsilon}_{\text{min}}). \tag{6}$$

Here parameter $\phi$ is analogous to the degree of polarization $A$, and $\sigma$ is a real quantity representing an arbitrary phase. Conveniently this can be represented by Fig. 1, where the electric field vector sweeps out an ellipse in a unit period about the axis of wave vector $\hat{k}$ with semimajor and semiminor axes of the ellipse aligned along $\hat{\epsilon}_{\text{maj}}$ and $\hat{\epsilon}_{\text{min}}$, respectively. The ratio of the semiminor width to semimajor width of the ellipse needs to be $\tan\phi$. Furthermore using Eqs. (3) and (6), one can express $\iota(\hat{\epsilon} \times \hat{\epsilon}^*) = A\hat{k}$, where $A = \sin 2\phi$. The biased magnetic field is along the quantization axis $\hat{e}_B$ and can technically be aligned in any direction. Without loss of generality, it can be assumed to lie in the $\hat{\epsilon}_{\text{maj}} \sim \hat{\epsilon}_{\text{min}}$ plane for the present requirement. Parameters $\theta_{\text{maj}}$, $\theta_{\text{min}}$, and $\theta_k$ are the angles between the respective unit vectors and $\hat{e}_B$, respectively, as shown in Fig. 1. In terms of these geometrical parameters,

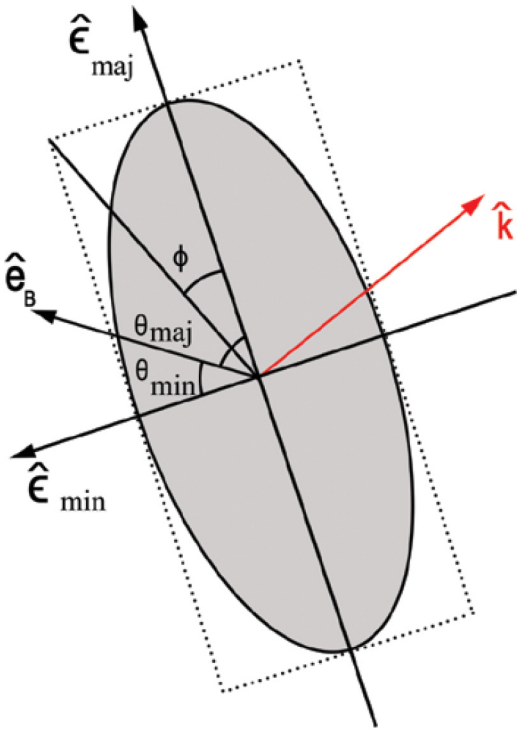


FIG. 1. Schematic representation of elliptically polarized light swept out by the polarization vector in one period. Unit vector $\hat{\epsilon}_{\text{maj}}$ ($\hat{\epsilon}_{\text{min}}$) aligns along the semimajor (semiminor) axis. The vectors $\hat{\epsilon}_{\text{maj}}$, $\hat{\epsilon}_{\text{min}}$, and $\hat{k}$ are mutually perpendicular to each other, while $\hat{e}_B$ is the quantization axis lying in the plane of $\hat{\epsilon}_{\text{maj}}$ and $\hat{\epsilon}_{\text{min}}$ and is perpendicular to $\hat{k}$.

one can conveniently express $\beta(\epsilon) = A\hat{k} \cdot \hat{e}_B = A\cos\theta_k$ and $\gamma(\epsilon) = \frac{1}{2}(3\cos^2\theta_p - 1)$, satisfying the relations

$$\cos^2\theta_p = \cos^2\phi\cos^2\theta_{\text{maj}} + \sin^2\phi\cos^2\theta_{\text{min}} \tag{7}$$

and

$$\theta_{\text{min}} + \theta_{\text{maj}} = 90^\circ. \tag{8}$$

Substituting the explicit form of $\beta(\epsilon)$ and $\gamma(\epsilon)$ in Eq. (2), the expression for the polarizability is given by

$$\begin{aligned}\alpha_K(\omega) = \alpha_K^{(0)}(\omega) &+ (A\cos\theta_k)\frac{M}{2K}\alpha_K^{(1)}(\omega) \\ &+\left(\frac{3\cos^2\theta_p - 1}{2}\right)\frac{3M^2 - K(K+1)}{K(2K-1)}\alpha_K^{(2)}(\omega). \end{aligned} \tag{9}$$

In this description, it reduces to $\beta(\epsilon) = 0$ and $\gamma(\epsilon) = \frac{1}{2}(3\cos^2\psi - 1)$ for the linearly polarized light with $\phi = 0$, where $\psi$ is the angle between the quantization axis and direction of polarization vector. Similarly, one can simplify the above expression for the circularly polarized light by using either $\phi = 45^\circ$ or $\phi = 135^\circ$.

To eliminate the dependence of $\lambda_{\text{magic}}$ on $M$ values in Eq. (5), one can choose a suitable combination of the above parameters so that null values for both $\beta(\epsilon) = A\cos\theta_k$ and $\gamma(\epsilon) = \frac{1}{2}(3\cos^2\theta_p - 1)$ can be achieved. This obviously corresponds to $\cos\theta_k = 0$ and $\cos^2\theta_p = \frac{1}{3}$, which can be brought about by suitably setting up the $\phi$, $\theta_k$, and $\theta_{\text{maj}}$ parameters. One can achieve $\cos\theta_k = 0$ by fixing the quantization axis

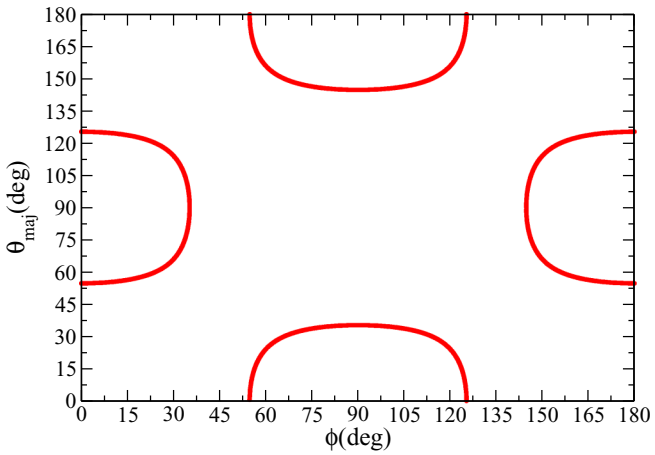


FIG. 2. Combinations of $\theta_{\rm maj}$ and $\phi$ values, marked with red curves, for which $\cos^2\theta_p = \frac{1}{3}$.

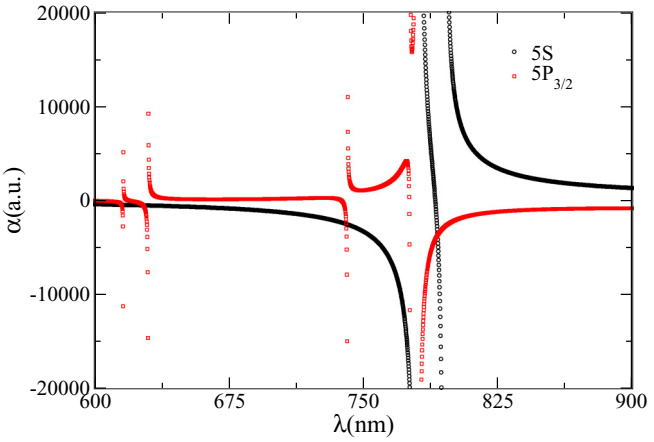


FIG. 3. $M_J$ independent dynamic polarizabilities (in a.u.) of the $5S$ and $5P_{3/2}$ states in Rb against wavelengths (in nm) for the proposed elliptically polarized light with $\cos\theta_k = 0$ and $\cos^2\theta_p = \frac{1}{3}$.

$\hat{e}_B$ at right angles to the wave vector; i.e. one can assume $e_B$ to repose in the $\hat{\epsilon}_{\rm maj} \sim \hat{\epsilon}_{\rm min}$ plane. On the other hand, many possible freedoms exist to achieve $\cos^2\theta_p = \frac{1}{3}$. For example, we plot $\theta_{\rm maj}$ values (note that $\theta_{\rm maj}$ and $\theta_{\rm min}$ are related) versus $\phi$ in Fig. 2, where each point on the graph represents a set of $\theta_{\rm maj}$ and $\phi$ that can yield $\cos^2\theta_p = \frac{1}{3}$. As mentioned previously, $\phi$ is a measure of the polarization and can be adjusted by setting the eccentricity $e$ of the ellipse ($|A| = \frac{2\sqrt{1-e^2}}{2-e^2}$). It is evident from Fig. 2 that for the values $\phi = 45^\circ$ and $135^\circ$, none of the pairs of angles $\phi$ and $\theta_{\rm maj}$ can offer $\cos^2\theta_p = \frac{1}{3}$. This means that the above criterion cannot be attained by applying the circularly polarized light. However, as has been reported in [28], this condition can be attained with $\phi = 0^\circ$ and $\psi = 54.74^\circ$ for a linearly polarized light. This critical condition seems to be too demanding and could be hard to achieve in an experimental set-up. On the other hand, one could get a more relaxed experimental conditions by using an elliptical polarized light as it offers more freedom to choose

TABLE I. Magic wavelengths $\lambda_{\rm magic}$ (in nm) with the corresponding polarizability $\alpha_v(\omega)$ (in atomic units) for the $5S - 5P_{3/2}$ and $6S - 6P_{3/2}$ transitions in the Rb and Cs atoms, respectively, with the proposed elliptically polarized light with $\cos\theta_k = 0$ and $\cos^2\theta_p = \frac{1}{3}$. In between resonant wavelengths $\lambda_{\rm res}$ (in nm) are also mentioned.

| Rb | | | | Cs | | | |
|---|---|---|---|---|---|---|---|
| Resonant transition | $\lambda_{\rm res}$ | $\lambda_{\rm magic}$ | $\alpha_v(\omega)$ | Resonant transition | $\lambda_{\rm res}$ | $\lambda_{\rm magic}$ | $\alpha_v(\omega)$ |
| $5P_{3/2} - 8D_{3/2}$ | 543.33 | | | $6P_{3/2} - 9D_{5/2}$ | 584.68 | | |
| | | 615.2 | −478 | | | 602.9 | −340 |
| $5P_{3/2} - 8S_{1/2}$ | 616.13 | | | $6P_{3/2} - 10S_{1/2}$ | 603.58 | | |
| | | 627.2 | −532 | | | 614.8 | −368 |
| $5P_{3/2} - 6D_{5/2}$ | 630.01 | | | $6P_{3/2} - 8D_{5/2}$ | 621.48 | | |
| $5P_{3/2} - 6D_{3/2}$ | 630.10 | | | | | 621.9 | −384 |
| | | 740.4 | −2515 | $6P_{3/2} - 8D_{3/2}$ | 621.93 | | |
| $5P_{3/2} - 7S_{1/2}$ | 741.02 | | | | | 657.7 | −502 |
| | | 775.8 | −20048 | $6P_{3/2} - 9S_{1/2}$ | 658.83 | | |
| $5P_{3/2} - 5D_{5/2}$ | 775.98 | | | | | 685.9 | −628 |
| $5P_{3/2} - 5D_{3/2}$ | 776.16 | | | $6P_{3/2} - 7D_{5/2}$ | 697.52 | | |
| $5P_{3/2} - 5S_{1/2}$ | 780.24 | | | | | 698.5 | −697 |
| | | 791.3 | −3681 | $6P_{3/2} - 7D_{3/2}$ | 698.54 | | |
| $5P_{3/2} - 6S_{1/2}$ | 1366.87 | | | | | 793.6 | −2094 |
| | | 1397.1 | 461 | $6P_{3/2} - 8S_{1/2}$ | 794.61 | | |
| $5P_{3/2} - 4D_{5/2}$ | 1529.26 | | | $6S_{1/2} - 6P_{3/2}$ | 852.35 | | |
| | | | | | | 886.4 | −3736 |
| | | | | $6S_{1/2} - 6P_{1/2}$ | 894.59 | | |
| | | | | $6P_{3/2} - 6D_{5/2}$ | 917.48 | | |
| | | | | | | 920.6 | 4131 |
| | | | | $6P_{3/2} - 6D_{3/2}$ | 921.11 | | |
| | | | | | | 936.2 | 2994 |
| | | | | $6P_{3/2} - 7S_{1/2}$ | 1469.89 | | |

from a number of $\phi$ and $\theta_{\rm maj}$ combinations as shown in Fig. 2. In fact, we observe that these estimated values of $\lambda_{\rm magic}$ will change maximum up to 1% for the variation of $\theta_{\rm maj}$ by one degree when $\phi$ is constant and vice versa. Therefore, it seems feasible to prepare a trap geometry using our proposed criteria for the elliptically polarized light aptly.

## IV. RESULTS

It looks straightforward to achieve $\lambda_{\rm magic}$ for any atomic or hyperfine transition in a given atomic system by maintaining the above geometry for trapping atoms provided that the differential polarizabilities of the considered transition nullifies within the resonance lines. We subsequently demonstrate below these $\lambda_{\rm magic}$, specifically for the $D_2$ lines of the Rb and Cs atoms.

*Rb atom.* In Fig. 3, we have plotted scalar dipole polarizabilities of the $5S$ and $5P_{3/2}$ states of Rb with respect to wavelength of the external electric field. These values were obtained in our previous work where we presented $\lambda_{\rm magic}$ for the $D$ lines of Rb using the linearly and circularly polarized light [9]. As can be seen from the figure, a number of $\lambda_{\rm magic}$ represented by the crossings of $5S$ and $5P_{3/2}$ polarizabilities have been predicted for this transition and are presented in Table I along with the resonance lines to highlight their locations. Two $\lambda_{\rm magic}$ are found at 615.2 and 627.2 nm, which belong to the visible region, while the other five $\lambda_{\rm magic}$ are located at 740.4, 775.8, 791.3, and 1397.1 nm. One more probable $\lambda_{\rm magic}$ in between the $5P_{3/2} - 6D_{5/2}$ and $5P_{3/2} - 6D_{3/2}$ resonance lines seems to exist, but we have not listed it in the table due to inability to identify it distinctly. All the $\lambda_{\rm magic}$ mentioned in Table I, except the one at 1397.1 nm, support the blue-detuned trapping scheme. We, however, recommend the use of $\lambda_{\rm magic}$ at 791.3 nm for a blue-detuned and 1397.1 nm for a red-detuned trap for experimental purposes, since these wavelengths are far from the resonant transitions.

*Cs atom.* Adopting a similar procedure as in Ref. [10], we have evaluated dynamic polarizabilities of the ground and $6P$ states of Cs. We have also plotted the frequency-dependent scalar polarizabilities of the ground and $6P_{3/2}$ states of this atom in Fig. 4 to find out $\lambda_{\rm magic}$ that are independent of the magnetic sublevels and hyperfine levels of the atomic states of the $D_2$ line. Table I lists the $\lambda_{\rm magic}$ for this transition which lie within the wavelength range of 600–1500 nm. As demonstrated in Ref. [10], $\lambda_{\rm magic}$ exist between every two resonances for the linearly polarized light. We correspondingly locate six wavelengths at 602.9, 614.8, 621.9, 657.7, 685.9, and 698.5 nm in the visible region using the proposed geometry

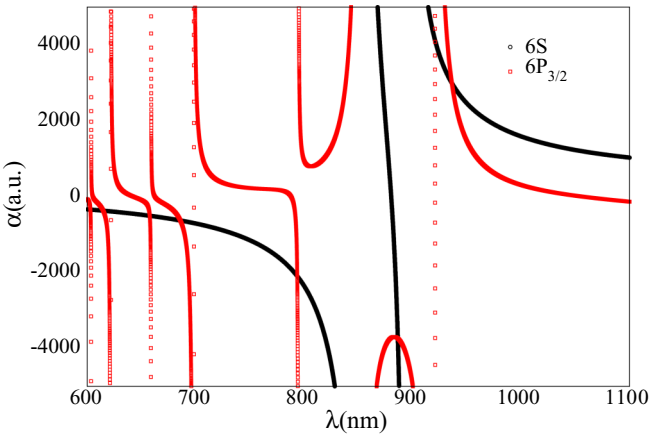


FIG. 4. $M_J$ independent dynamic polarizabilities (in a.u.) of the $6S$ and $6P_{3/2}$ states in Cs against wavelengths (in nm) for the proposed elliptically polarized light with $\cos\theta_k = 0$ and $\cos^2\theta_p = \frac{1}{3}$.

for an elliptically polarized light. We also found two $\lambda_{\rm magic}$ at 793.6 and 886.4 nm, which belong to infrared region. They all support dark or blue-detuned traps. Two more $\lambda_{\rm magic}$ in the infrared region are located at 920.6 and 936.2 nm that can support red-detuned traps. In this case, we intend to recommend the use of $\lambda_{\rm magic}$ at 920.6 and 936.2 nm for the red-detuned trapping and 685.9 nm for the blue-detuned trapping due to the availability of lasers at these wavelengths.

## V. CONCLUSION

A trap geometry has been proposed using an elliptically polarized light in a sufficiently large magnetic field that can produce null differential ac-Stark shifts among the transitions and can be exclusively applicable among any magnetic sublevels and hyperfine levels. Their applications in the $D_2$ lines of Rb and Cs atoms have been highlighted and the corresponding magic wavelengths are reported. Furthermore, we have also recommended the magic wavelengths that are suitable for both the blue- and red-detuned traps of Rb and Cs atoms. These magic wavelengths will be immensely useful in a number of high-precision measurements.

## ACKNOWLEDGMENTS

We gratefully acknowledge helpful discussions with Dr. K. Beloy, Jasmeet Kaur, and Kiranpreet Kaur. S.S. acknowledges financial support from the UGC-BSR scheme. The work of B.A. is supported by CSIR Grant No. 03(1268)/13/EMR-II, India.

[1] C. S. Wood, S. C. Bennett, D. Cho, B. P. Masterson, J. L. Roberts, C. E. Tanner, and C. E. Wieman, Science **275**, 1759 (1997).
[2] T. Pruttivarasin, M. Ramm, S. G. Porsev, I. I. Tupitsyn, M. S. Safronova, M. A. Hohensee, and H. Haffner, Nature **517**, 592 (2015).
[3] T. G. Tiecke, J. D. Thompson, N. P. de Leon, L. R. Liu, V. Vuletic, and M. D. Lukin, Nature **508**, 241 (2014).
[4] U. Vogl and M. Weitz, Nature **461**, 70 (2009).
[5] C. Monroe, H. Robinson, and C. Wieman, Opt. Lett. **16**, 50 (1991).
[6] H. Katori, T. Ido, and M. Kuwata-Gonokami, J. Phys. Soc. Jpn. **68**, 2479 (1999).
[7] N. Lundblad, M. Schlosser, and J. V. Porto, Phys. Rev. A **81**, 031611 (2010).
[8] M. S. Safronova, U. I. Safronova, and C. W. Clark, Phys. Rev. A **86**, 042505 (2012).

[9] B. K. Sahoo and B. Arora, Phys. Rev. A **87**, 023402 (2013).
[10] B. Arora, M. S. Safronova, and C. W. Clark, Phys. Rev. A **76**, 052509 (2007).
[11] M. Takamoto, F. L. Hong, R. Higashi, and H. Katori, Nature **435**, 321 (2005).
[12] L. Yi, S. Mejri, J. J. McFerran, Y. LeCoq, and S. Bize, Phys. Rev. Lett. **106**, 073005 (2011).
[13] Z. W. Barber, C. W. Hoyt, C. W. Oates, L. Hollberg, A. V. Taichenachev, and V. I. Yudin, Phys. Rev. Lett. **96**, 083002 (2006).
[14] V. D. Ovsiannikov, V. G. Palchikov, A. V. Taichenachev, V. I. Yudin, H. Katori, and M. Takamoto, Phys. Rev. A **75**, 020501 (2007).
[15] Y. B. Tang, H. X. Qiao, T. Y. Shi, and J. Mitroy, Phys. Rev. A **87**, 042517 (2013).
[16] J. Kaur, S. Singh, B. Arora, and B. K. Sahoo, Phys. Rev A **92**, 031402(R) (2015).
[17] M. Takamoto and H. Katori, Phys. Rev. Lett. **91**, 223001 (2003).
[18] J. McKeever, J. R. Buck, A. D. Boozer, A. Kuzmich, H.-C. Nagerl, D. M. Stamper-Kurn, and H. J. Kimble, Phys. Rev. Lett. **90**, 133602 (2003).
[19] P.-L. Liu, Y. Huang, W. Bian, H. Shao, H. Guan, Y.-B.Tang, C.-B. Li, J. Mitroy, and K.-L. Gao, Phys. Rev. Lett. **114**, 223001 (2015).
[20] B. Arora and B. K. Sahoo, Phys. Rev. A **86**, 033416 (2012).
[21] R. W. Fox, S. L. Gilbert, L. Hollberg, J. H. Marquardt, and H. G. Robinson, Opt. Lett. **18**, 1456 (1993).
[22] B. Yang, Q. Liang, J. He, and J. Wang, Opt. Express **20**, 11944 (2012).
[23] V. M. Entin and I. I. Ryabtsev, J. Exp. Theor. Phys. Lett. **80**, 161 (2004).
[24] S. Friebel, C. D'Andrea, J. Walz, M. Weitz, and T. W. Hansch, Phys. Rev. A **57**, R20(R) (1998).
[25] V. Gerginov, K. Calkins, C. E. Tanner, J. J. McFerran, S. Diddams, A. Bartels, and L. Hollberg, Phys. Rev. A **73**, 032504 (2006).
[26] N. L. Manakov, V. D. Ovsiannikov, and L. P. Rapoport, Phys. Rep. **141**, 320 (1986).
[27] K. Beloy, Theory of the ac stark effect on the atomic hyperfine structure and applications to microwave atomic clocks, Ph.D. thesis, University of Nevada, Reno, USA, 2009.
[28] S. Kotochigova and D. DeMille, Phys. Rev. A **82**, 063421 (2010).